Appendix

An Engineered Multicellular Stem Cell Niche for the 3D Derivation of Human Myogenic Progenitors from iPSCs

Omid Mashinchian, Filippo De Franceschi, Sina Nassiri, Joris Michaud, Eugenia Migliavacca, Patrick Aouad, Sylviane Metairon, Solenn Pruvost, Sonia Karaz, Paul Fabre, Thomas Molina, Pascal Stuelsatz, Nagabhooshan Hegde, Emmeran Le Moal, Gabriele Dammone, Nicolas A. Dumont, Matthias P. Lutolf, Jerome N. Feige, C. Florian Bentzinger

Table of contents

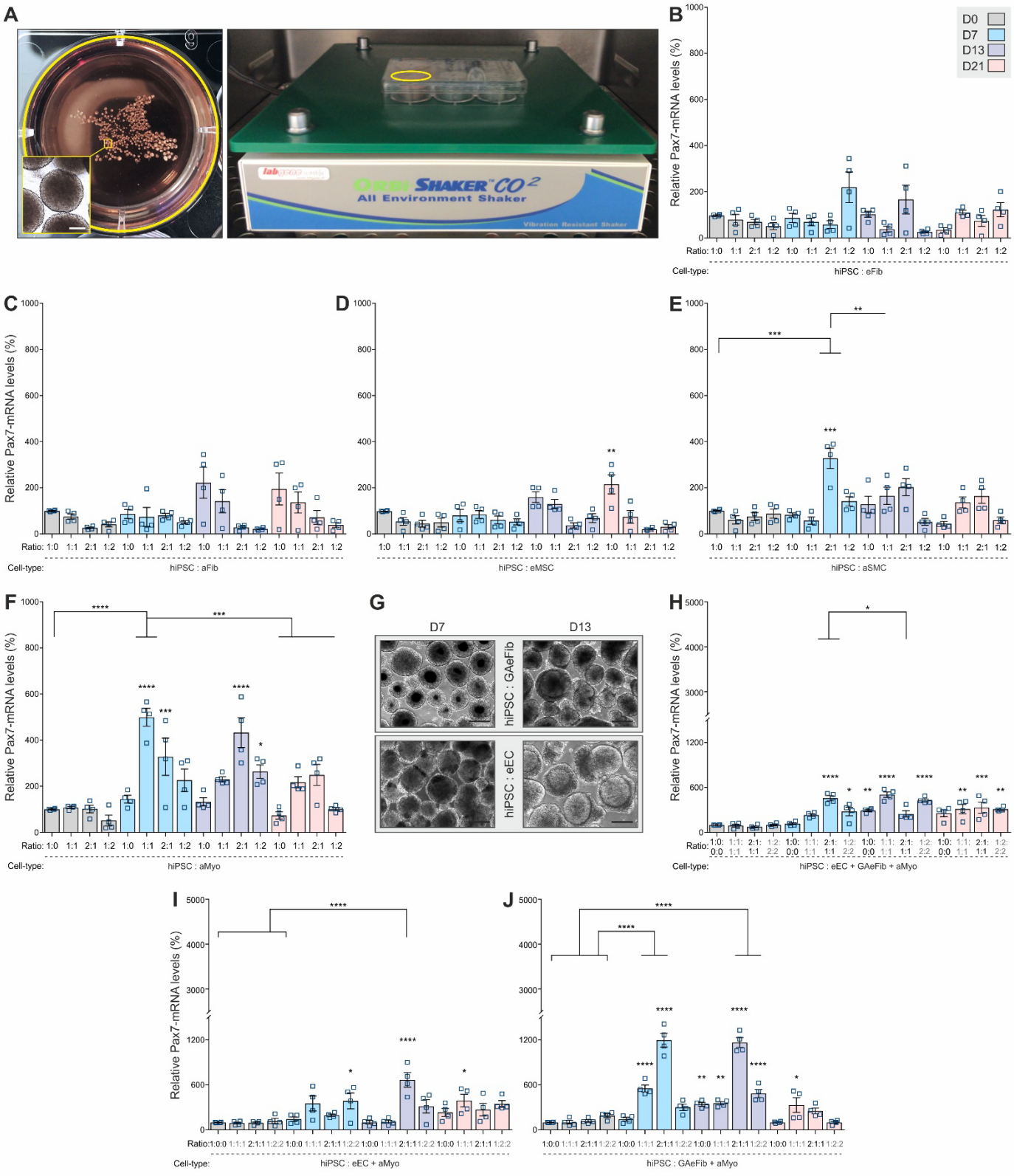
A
B
Relative Pax7-mRNA levels (%)
D0
D7
D13
D21
Ratio: 1:0 1:1 2:1 1:2 1:0 1:1 2:1 1:2 1:0 1:1 2:1 1:2 1:0 1:1 2:1 1:2
Cell-type:
hiPSC : eFib
C
hiPSC : aFib
D
hiPSC : eMSC
E
hiPSC : aSMC
F
hiPSC : aMyo
G
D7
D13
hiPSC : GAeFib
hiPSC : eEC
H
hiPSC : eEC + GAeFib + aMyo
I
hiPSC : eEC + aMyo
J
hiPSC : GAeFib + aMyo

Appendix Figure S1: Characterization of multi-component embryoids. A. Horizontal shaker platform setup used to generate multi-component embryoids. Scale bar = 50 µm. **B-F.** mRNA expression of Pax7 in embryoids containing different ratios of hiPSCs and embryonic fibroblasts (eFib), adult fibroblasts (aFib), embryonic mesenchymal-like stem cells (eMSC), adult smooth muscle cells (aSMC) or adult myoblasts (aMyo). Mixtures of the respective cell types were interrogated before (D0), and at 7, 13, and 21 days (D7, D13, D21) after aggregation. **G.** Representative brightfield images of embryoids containing hiPSCs and embryonic endothelial cells (eEC) or growth-arrested embryonic fibroblasts (GAeFib) in a 2:1 ratio at D7 and D13. Scale bars = 125µm. **H-J.** mRNA expression of Pax7 in embryoids containing different ratios of hiPSCs, GAeFib, eEC, aMyo. Mixtures of the respective cell types were interrogated before (D0), and at 7, 13, and 21 days (D7, D13, D21) after aggregation. **B-F,H-J**. Data are represented as means ± S.E.M from n=4 independent experiments. **A-J.** hiPSC donor 1. p-values are *p<0.05, **p<0.01, ***p<0.001, ****p<0.0001 using ANOVA followed by a Bonferroni post hoc test.

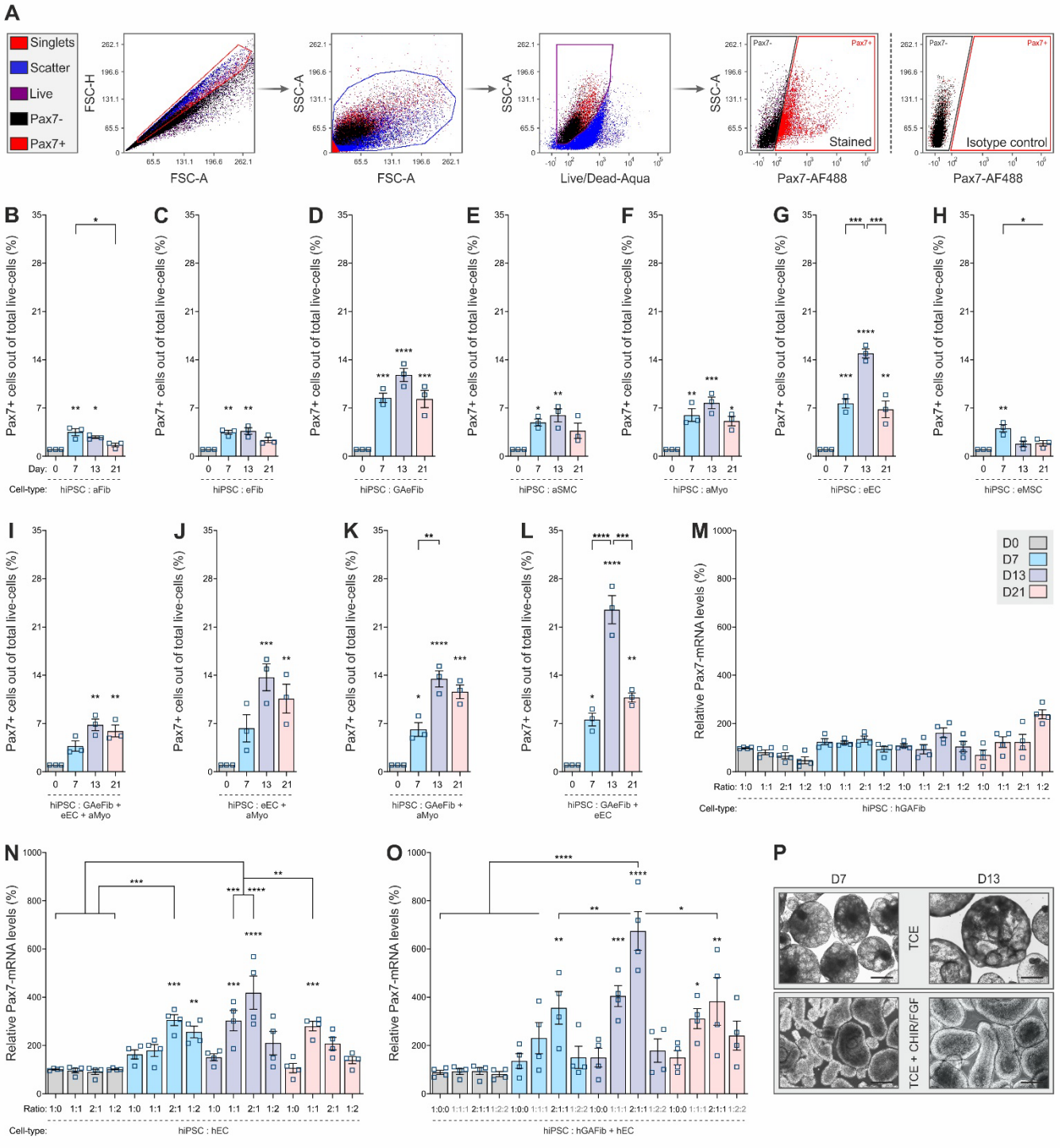
A
Singlets
Scatter
Live
Pax7-
Pax7+
FSC-H
FSC-A
SSC-A
FSC-A
SSC-A
Live/Dead-Aqua
SSC-A
Pax7-AF488
Stained
Isotype control
Pax7-AF488
B
C
D
E
F
G
H
Pax7+ cells out of total live-cells (%)
Day: 0 7 13 21
Cell-type:
hiPSC : aFib
hiPSC : eFib
hiPSC : GAeFib
hiPSC : aSMC
hiPSC : aMyo
hiPSC : eEC
hiPSC : eMSC
I
J
K
L
M
hiPSC : GAeFib + eEC + aMyo
hiPSC : eEC + aMyo
hiPSC : GAeFib + aMyo
hiPSC : GAeFib + eEC
Relative Pax7-mRNA levels (%)
D0
D7
D13
D21
Ratio: 1:0 1:1 2:1 1:2
hiPSC : hGAFib
N
O
P
hiPSC : hEC
hiPSC : hGAFib + hEC
D7
D13
TCE
TCE + CHIR/FGF

Appendix Figure S2: Flow cytometry quantification of Pax7 positive cells in multicellular embryoids and Pax7 expression in xeno-free TCEs. A. Flow cytometry gating strategy for quantification of Pax7 positive cells from three-component embryoids (TCEs). **B-L.** Repeat of the screen shown in Fig 1A-D and Appendix Fig S1A-J using an alternative hiPSC donor cell line at a 2:1 ratio of hiPSCs and the different cell types quantified by flow cytometry assessment of Pax7 positive cells. Four or three component embryoids were analyzed at a 2:1:1:1 respectively a 2:1:1 ratio of hiPSCs to different cell types. Embryoids containing hiPSCs and adult fibroblasts (aFib), embryonic fibroblasts (eFib), growth-arrested embryonic fibroblasts (GAeFib), adult smooth muscle cells (aSMC), adult skeletal muscle myoblasts (aMyo), embryonic endothelial cells (eEC), or embryonic mesenchymal-like stem cells (eMSC) were analyzed before (D0), and at 7, 13, and 21 days (D7, D13, D21) after aggregation. **M-O.** mRNA expression of Pax7 in xeno-free embryoids containing different ratios of hiPSCs, human growth-arrested fibroblasts (hGAFib), and human endothelial cells (hEC). Mixtures of the respective cell types were interrogated before (D0), and at 7, 13, and 21 days (D7, D13, D21) after aggregation. **P.** Representative brightfield images of TCEs containing hiPSCs, eEC, and GAeFib in a 2:1:1 ratio with and without stimulation of the Wnt/FGF pathways. Scale bars = 125μm. **B-O**. Data are represented as means ± S.E.M from n=3 (**B-L**) and n=4 (**M-N**) independent experiments. **A.** hiPSC donor 1**. B-L.** hiPSC donor 2, **M-P.** hiPSC donor 1. p-values are *p<0.05, **p<0.01, ***p<0.001, ****p<0.0001 using ANOVA followed by a Bonferroni post hoc test.

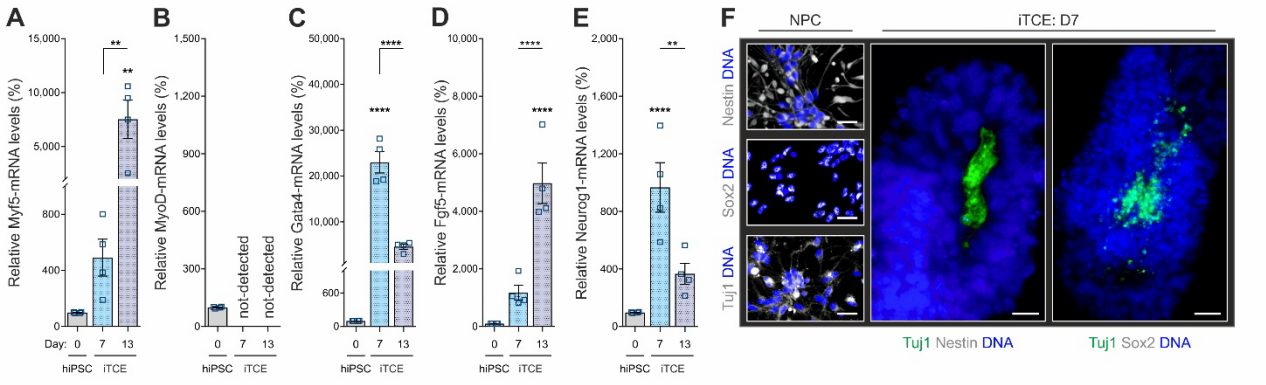

Appendix Figure S3: Myogenic commitment factors, endodermal, and ectodermal markers in TCEs. A-E. mRNA expression of the myogenic commitment markers Myf5 and MyoD, the endoderm marker Gata4, and the ectoderm markers Fgf5 and neurog1 in hiPSCs and Wnt/FGF induced TCEs (iTCEs) at D7 and D13. **F.** Representative stainings for the neuronal progenitor markers Tuj1, Nestin, and Sox2 in Wnt pathway induced D7 iTCEs. Human neural progenitor cells (NPCs) are shown as a positive control. Scale bars in the three left-hand side images = 25µm, scale bar on the two larger right-hand side images = 20µm. **A-E.** Data are represented as means ± S.E.M from n=4 independent experiments. **A-F.** hiPSC donor 1. p-values are *p<0.05, **p<0.01, ***p<0.001, ****p<0.0001 using an ANOVA followed by a Bonferroni post hoc test.

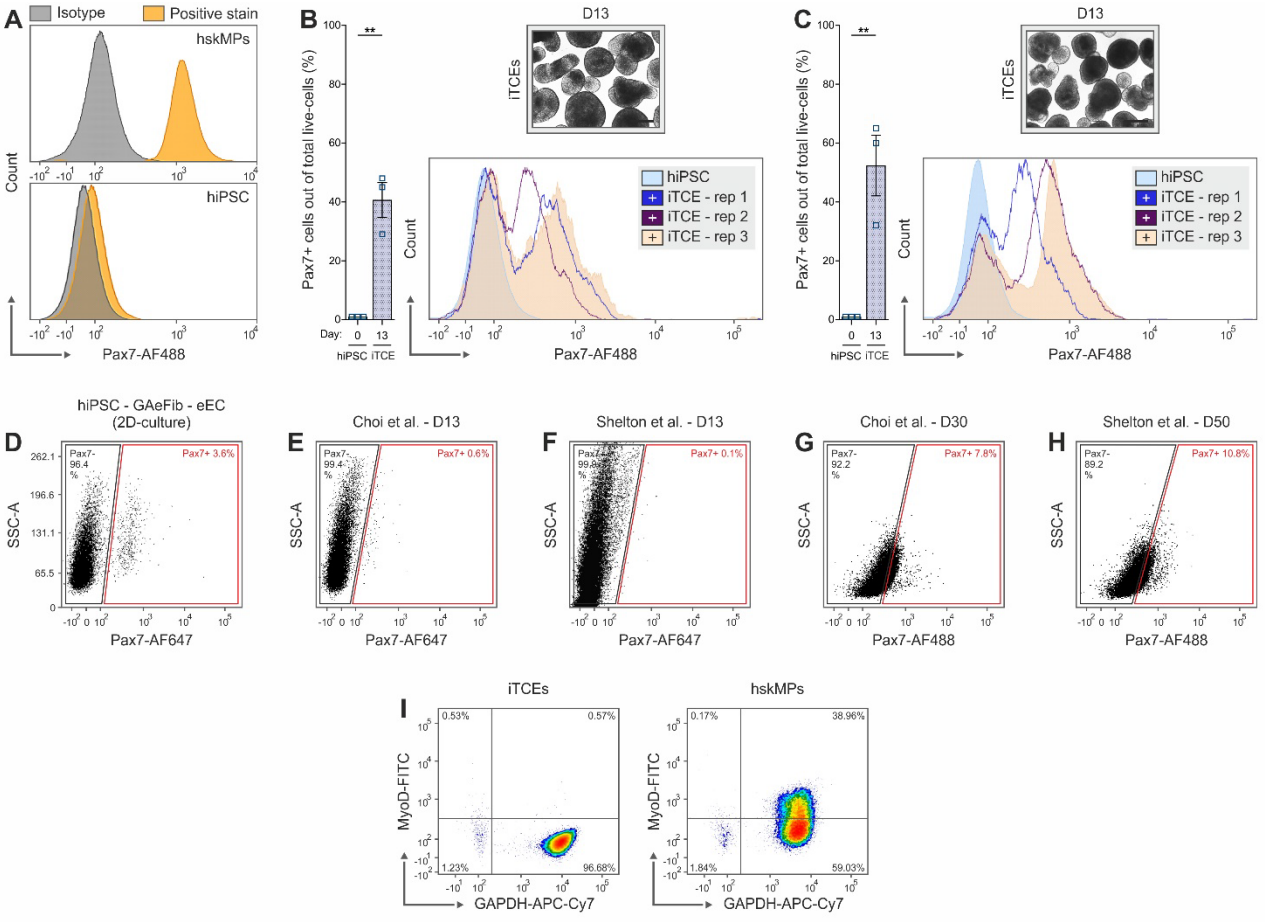

Appendix Figure S4: Flow cytometry validation and comparison of established 2D protocols for myogenic hiPSC differentiation with embryoid derivation. A. Flow cytometry validation of the Pax7 antibody using hiPSCs and hskMPs. **B,C.** Flow cytometry quantification of Pax7 positive cells from day 13 (D13) iTCEs containing hiPSCs lines from donor 2 (b) and donor 3 (c) with representative images. As a control, hiPSCs before aggregation (D0) are shown. **D.** Flow cytometry quantification of Pax7 in hiPSCs co-cultured with GAeFib and eEC in 2D over two weeks. Wnt pathway activation was induced from day 1-7 and bFGF stimulation from day 7-13. **E,F.** Flow cytometry quantification for Pax7 in hiPSC cultures differentiated for two weeks according to Choi or Shelton et al. (Choi et al., 2016, Shelton et al., 2014). **G,H.** Flow cytometry quantification for Pax7 with the Choi and Shelton protocols completed at day 30 (D30) and day 50 (D50), respectively. **I,** RNA fluorescence in situ hybridization for the myogenic commitment marker MyoD and the positive control GAPDH in hskMPs and cells derived from D13 iTCEs quantified by flow cytometry. **B,C.** Data are represented as means ± S.E.M from n=3 independent experiments. **D-I.** Representative sorts of n≥3 repeats are provided in Appendix Table S1 and S3. **A,D-I.** hiPSC donor 1**. B.** hiPSC donor 2. **C.** hiPSC donor 3. p-values are *p<0.05, **p<0.01, ***p<0.001, ****p<0.0001 using a students t-test.

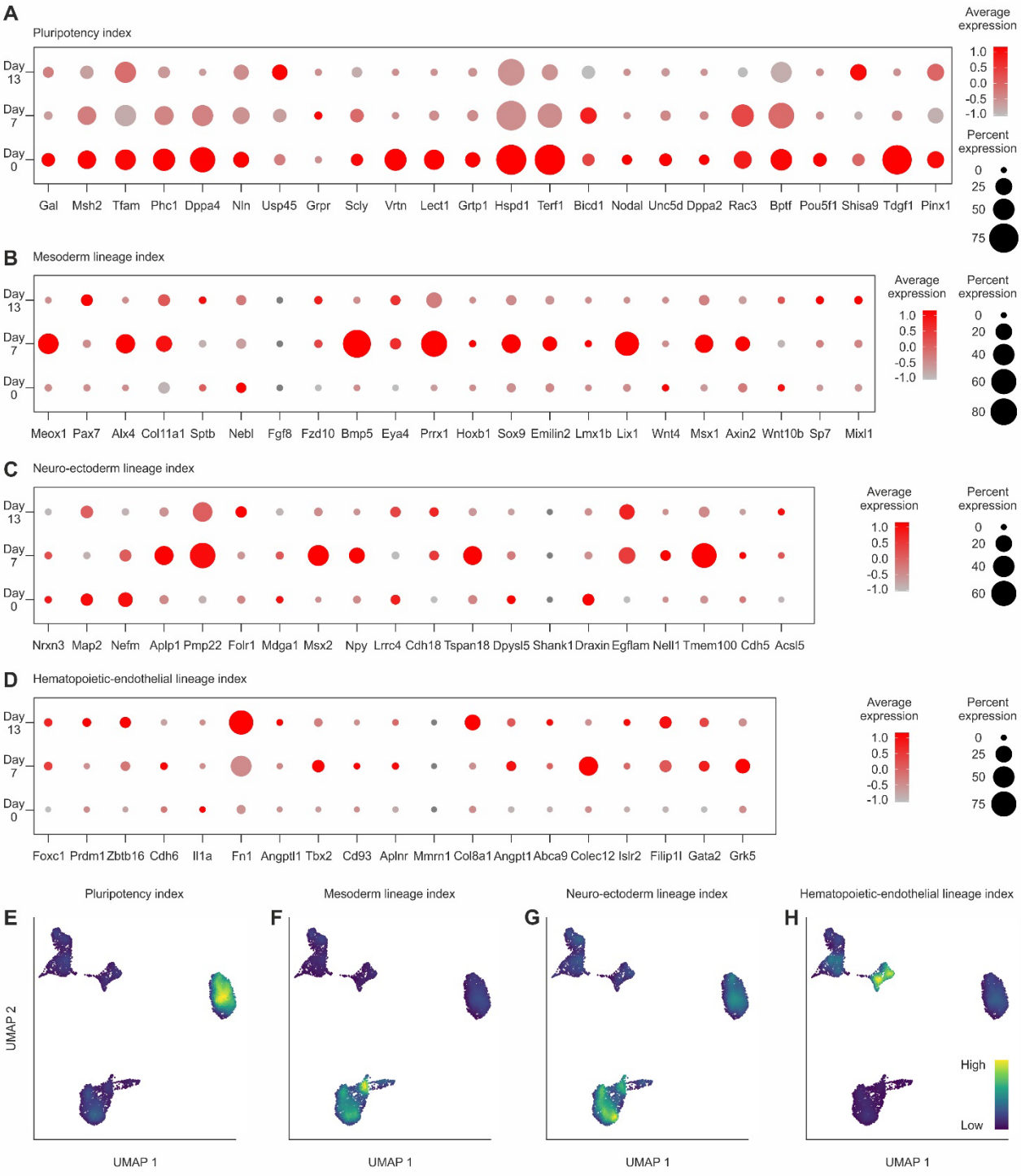

Appendix Figure S5: Expression of pluripotency and lineage markers during iTCE differentiation. A-D. Gene expression dot plots of single cells before aggregation (day 0), and from day 7 and 13 iTCEs visualizing the pluripotency, mesodermal, neuro-ectodermal, and hematopoietic-endothelial lineage index. **E-F.** 2D UMAP projection visualizing human single-cell transcriptomes of day 0, 7, and 13 iTCEs overlaid with the joint gene density of the pluripotency, mesodermal, neuro-ectodermal, and hematopoietic-endothelial lineage index. **A-H.** hiPSC donor 1.

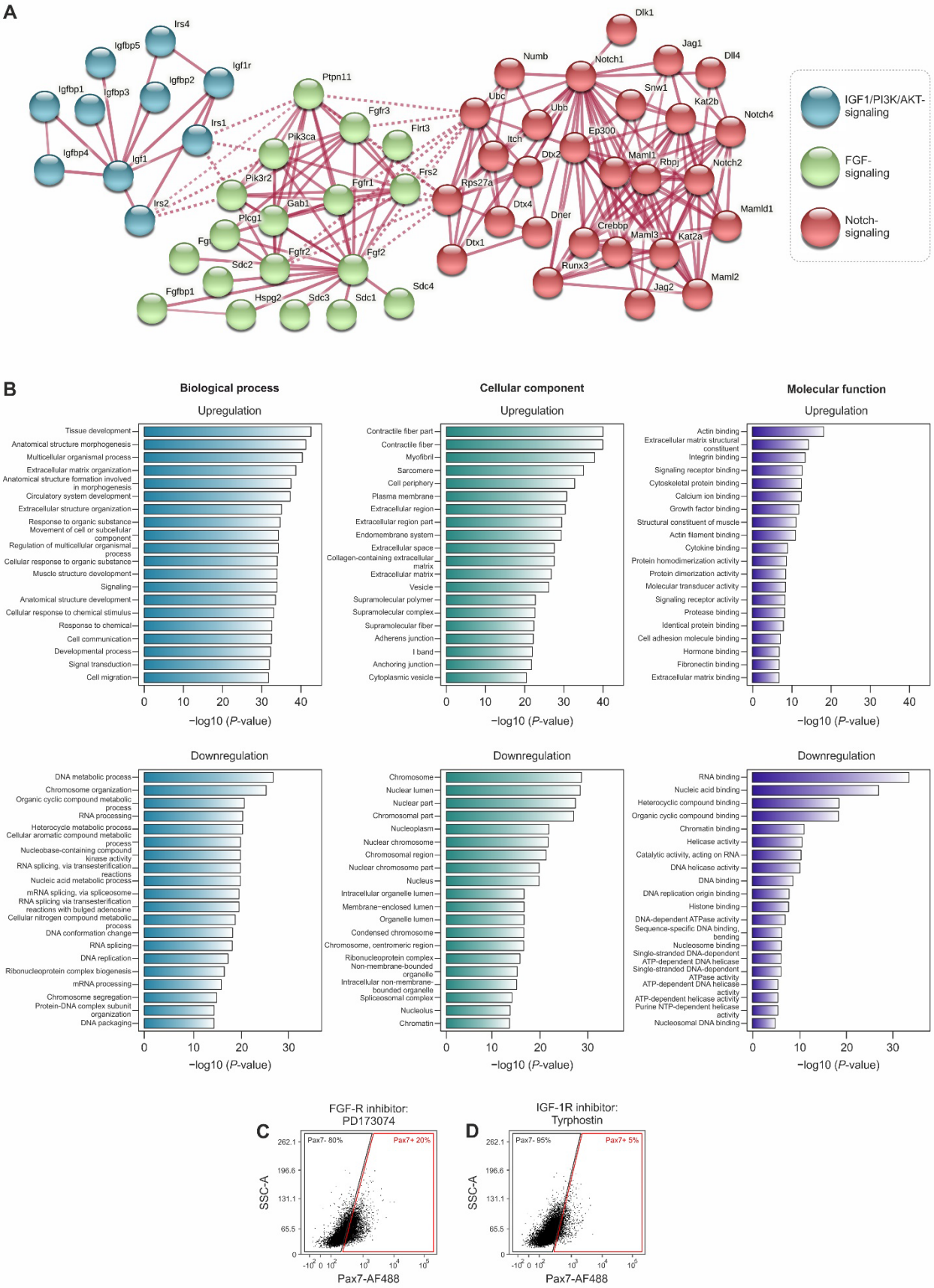
A
Irs4
Igfbp5
Igf1r
Igfbp2
Igfbp1
Igfbp3
Ptpn11
Irs1
Fgfr3
Flrt3
Pik3ca
Igfbp4
Igf1
Pik3r2
Fgfr1
Frs2
Irs2
Gab1
Plcg1
Fgf
Fgfr2
Fgf2
Sdc2
Fgfbp1
Hspg2
Sdc3
Sdc1
Sdc4
Dlk1
Jag1
Dll4
Numb
Notch1
Snw1
Ubc
Ubb
Kat2b
Notch4
Itch
Ep300
Dtx2
Maml1
Rbpj
Notch2
Rps27a
Dtx4
Dner
Mamld1
Crebbp
Maml3
Kat2a
Dtx1
Runx3
Maml2
Jag2
IGF1/PI3K/AKT-signaling
FGF-signaling
Notch-signaling
B
Biological process
Cellular component
Molecular function
Upregulation
Tissue development
Anatomical structure morphogenesis
Multicellular organismal process
Extracellular matrix organization
Anatomical structure formation involved in morphogenesis
Circulatory system development
Extracellular structure organization
Response to organic substance
Movement of cell or subcellular component
Regulation of multicellular organismal process
Cellular response to organic substance
Muscle structure development
Signaling
Anatomical structure development
Cellular response to chemical stimulus
Response to chemical
Cell communication
Developmental process
Signal transduction
Cell migration
Contractile fiber part
Contractile fiber
Myofibril
Sarcomere
Cell periphery
Plasma membrane
Extracellular region
Extracellular region part
Endomembrane system
Extracellular space
Collagen-containing extracellular matrix
Extracellular matrix
Vesicle
Supramolecular polymer
Supramolecular complex
Supramolecular fiber
Adherens junction
I band
Anchoring junction
Cytoplasmic vesicle
Actin binding
Extracellular matrix structural constituent
Integrin binding
Signaling receptor binding
Cytoskeletal protein binding
Calcium ion binding
Growth factor binding
Structural constituent of muscle
Actin filament binding
Cytokine binding
Protein homodimerization activity
Protein dimerization activity
Molecular transducer activity
Signaling receptor activity
Protease binding
Identical protein binding
Cell adhesion molecule binding
Hormone binding
Fibronectin binding
Extracellular matrix binding
0 10 20 30 40
−log10 (P-value)
Downregulation
DNA metabolic process
Chromosome organization
Organic cyclic compound metabolic process
RNA processing
Heterocycle metabolic process
Cellular aromatic compound metabolic process
Nucleobase-containing compound kinase activity
RNA splicing, via transesterification reactions
Nucleic acid metabolic process
mRNA splicing, via spliceosome
RNA splicing via transesterification reactions with bulged adenosine
Cellular nitrogen compound metabolic process
DNA conformation change
RNA splicing
DNA replication
Ribonucleoprotein complex biogenesis
mRNA processing
Chromosome segregation
Protein-DNA complex subunit organization
DNA packaging
Chromosome
Nuclear lumen
Nuclear part
Chromosomal part
Nucleoplasm
Nuclear chromosome
Chromosomal region
Nuclear chromosome part
Nucleus
Intracellular organelle lumen
Membrane−enclosed lumen
Organelle lumen
Condensed chromosome
Chromosome, centromeric region
Ribonucleoprotein complex
Non-membrane-bounded organelle
Intracellular non-membrane-bounded organelle
Spliceosomal complex
Nucleolus
Chromatin
RNA binding
Nucleic acid binding
Heterocyclic compound binding
Organic cyclic compound binding
Chromatin binding
Helicase activity
Catalytic activity, acting on RNA
DNA helicase activity
DNA binding
DNA replication origin binding
Histone binding
DNA-dependent ATPase activity
Sequence-specific DNA binding, bending
Nucleosome binding
Single-stranded DNA-dependent ATP-dependent DNA helicase
Single-stranded DNA-dependent ATPase activity
ATP-dependent DNA helicase activity
ATP-dependent helicase activity
Purine NTP-dependent helicase activity
Nucleosomal DNA binding
0 10 20 30
−log10 (P-value)
C
FGF-R inhibitor: PD173074
Pax7- 80%
Pax7+ 20%
SSC-A
262.1
196.6
131.1
65.5
0
Pax7-AF488
D
IGF-1R inhibitor: Tyrphostin
Pax7- 95%
Pax7+ 5%
SSC-A
262.1
196.6
131.1
65.5
0
Pax7-AF488

Appendix Figure S6: Signaling mechanisms in iTCEs. A. String network of extracellular ligands involved in the IGF/PI3K/AKT, FGF, and Notch pathways highly expressed in iTCEs. Nodes with an interaction score >0.7 are represented and colored according to pathways using an inflation parameter of 3. **B.** Go-analysis of the top 20 up- or downregulated categories in the biological process, cellular component, and molecular function ontologies in iTCEs compared to Wnt/FGF stimulated hiPSC mono-aggregates. **C,D.** Flow cytometry quantification for Pax7 in D13 iTCEs incubated with an FGF-receptor (FGF-R) and an IGF1-receptor (IGF-1R) inhibitor. Representative sorts of n$\geqslant$3 repeats are provided in Appendix Table S5. **A-D.** hiPSC donor 1.

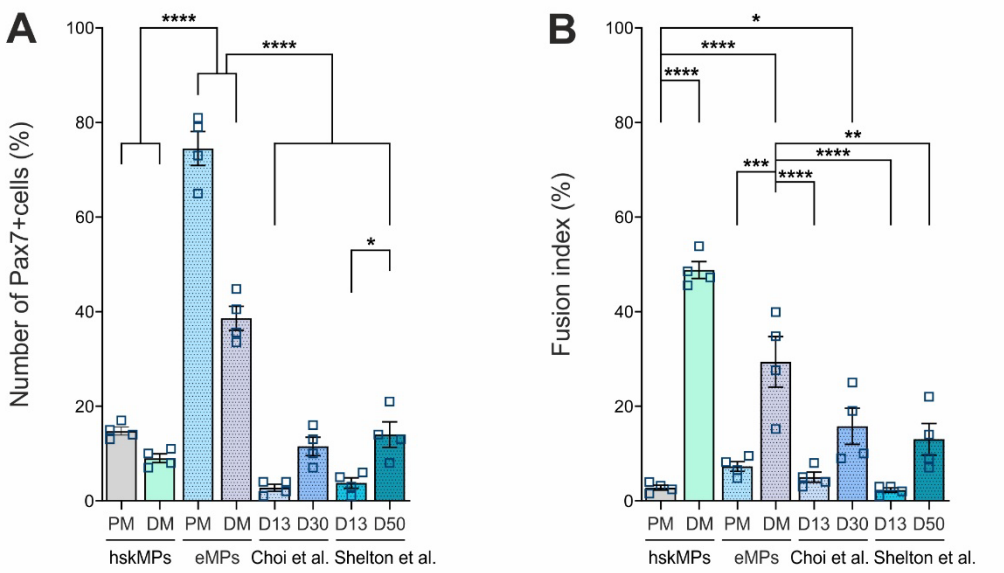

Appendix Figure S7: Comparison of established 2D protocols for myogenic hiPSC differentiation with eMPs. A. Quantification of the number of Pax7 positive cells in cultures of primary human skeletal muscle progenitors (hskMPs) and embryonic-like myogenic progenitors (eMPs) that were flow cytometrically isolated from iTCEs in proliferation (PM) and differentiation (DM) medium, as well as in hiPSC cultures differentiated according to Choi or Shelton et al. (Choi et al., 2016, Shelton et al., 2014) at two weeks (D13) and at the endpoint of the respective protocols at day 30 (D30) and day 50 (D50). **B.** Quantification of the fusion index in cultures of hskMPs and eMPs that were flow cytometrically isolated from iTCEs in PM and DM, as well as in hiPSC cultures differentiated according to Choi or Shelton et al. at D13 and at the endpoint of the respective protocols at D30 and D50. Data are represented as means ± S.E.M from n=4 independent experiments. **A,B.** hiPSC donor 1. p-values are *p<0.05, **p<0.01, ***p<0.001, ****p<0.0001 using an ANOVA followed by a Bonferroni post hoc test.

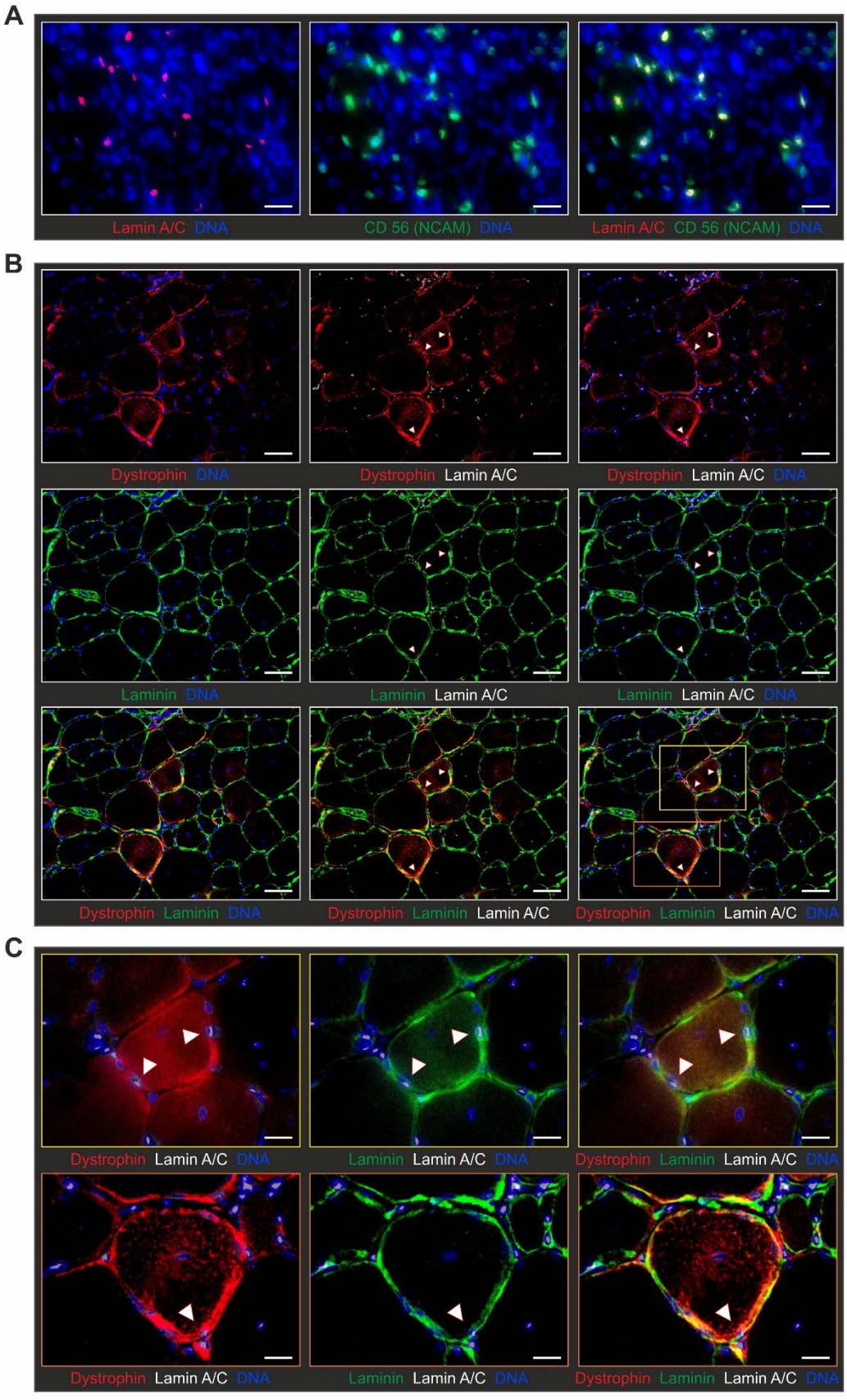
A
Lamin A/C DNA
CD 56 (NCAM) DNA
Lamin A/C CD 56 (NCAM) DNA
B
Dystrophin DNA
Dystrophin Lamin A/C
Dystrophin Lamin A/C DNA
Laminin DNA
Laminin Lamin A/C
Laminin Lamin A/C DNA
Dystrophin Laminin DNA
Dystrophin Laminin Lamin A/C
Dystrophin Laminin Lamin A/C DNA
C
Dystrophin Lamin A/C DNA
Laminin Lamin A/C DNA
Dystrophin Laminin Lamin A/C DNA
Dystrophin Lamin A/C DNA
Laminin Lamin A/C DNA
Dystrophin Laminin Lamin A/C DNA

Appendix Figure S8: Characterization of eMP engraftment in mdx mice. A. Representative immunostainings for human nuclear marker lamin A/C and CD56 in cross-sections of muscles of mdx mice after transplantation of eMPs. Scale bars = 25µm. **B,C.** Representative immunostainings for lamin A/C, dystrophin, and laminin in cross-sections of muscles of mdx mice after transplantation of eMPs. Arrowheads show lamin A/C positive cells in the satellite cell position in the periphery of dystrophin positive fibers. **B.** Scale bars = 50µm. **C.** Scale bars = 25 µm. **A-C.** 25 days post-transplantation.

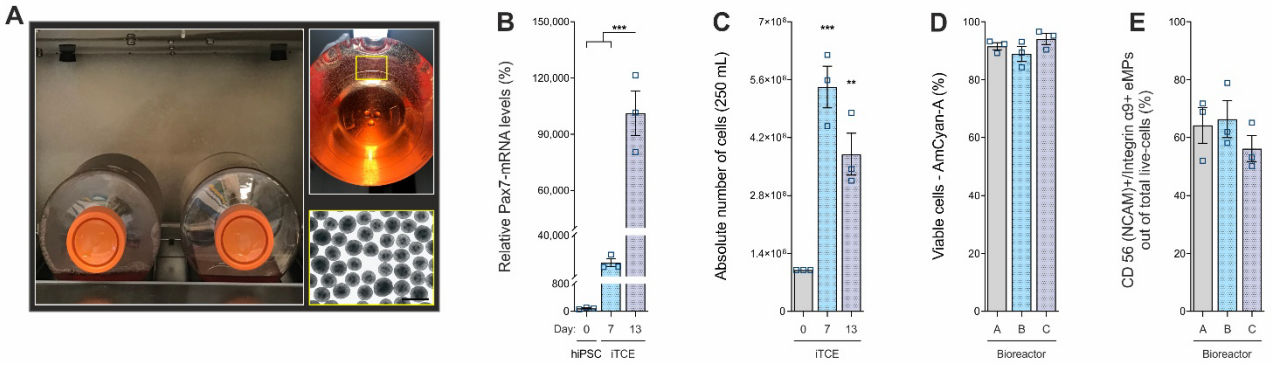

Appendix Figure S9: iTCE scale-up culture in roller bottles. A. Representative images of roller-bottle cultures and iTCEs generated using this system. **B.** mRNA expression of Pax7 in hiPSCs before aggregation (D0) and iTCEs at D7 and D13. **C.** Absolute number of cells before aggregation (D0) and iTCEs at D7 and D13 quantified by trypan blue staining. **D.** Calcein-AM and ethidium homodimer-1 based flow cytometric assessment of cell viability across different roller bottle bioreactors containing iTCEs after 13 days of culture. **E.** Flow cytometry quantification of the percentage of embryonic-like myogenic progenitors (eMPs) isolated using CD56 and integrin α9 across different roller bottle bioreactors containing iTCEs after 13 days of culture. **A.** Scale bar = 125μm**. B-E.** Data are represented as means ± S.E.M from n=3 independent experiments. **A-E.** hiPSC donor 1. p-values are *p<0.05, **p<0.01, ***p<0.001, ****p<0.0001 using ANOVA followed by a Bonferroni post hoc test.

2D-protocols	hiPSC - GAeFib - eEC (2D-culture)	Choi et al. - D13	Shelton et al. - D13	Choi et al. - D30	Shelton et al. - D50
Pax7+: Rep 1.	3.61	0.6	0.1	8.6	9.78
Pax7+: Rep 2.	2.87	0.68	0.18	7.8	9.75
Pax7+: Rep 3.	2.59	0.89	1.1	3.92	10.81
Pax7-: Rep 1.	96.39	99.4	99.9	91.4	90.22
Pax7-: Rep 2.	97.13	99.32	99.82	92.2	90.25
Pax7-: Rep 3.	97.41	99.11	98.9	96.08	89.19

Appendix Table S1: Flow cytometry quantification for Appendix Fig S4D-H. The table shows the results of 3 independent experimental repeats (Rep) in percent of total cells.

RNA-FISH probes	MyoD-FITC+ / Myf5-APC+	MyoD-FITC+	Myf5-APC+
iTCEs: Rep 1.	0.84	0.03	15.57
iTCEs: Rep 2.	1.12	0.08	15.11
iTCEs: Rep 3.	0.69	0.7	13.89
hskMPs: Rep 1.	40.92	1.27	53.01
hskMPs: Rep 2.	43.18	1.81	50.81
hskMPs: Rep 3.	41.19	0.9	54.18

Appendix Table S2: Flow cytometry quantification for Figure 1R and S. The table shows the results of 3 independent experimental repeats (Rep) in percent of total cells.

RNA-FISH probes	MyoD-FITC+ / GAPDH-APC-Cy7	MyoD-FITC+	GAPDH-APC-Cy7
iTCEs: Rep 1.	0.57	0.53	96.68
iTCEs: Rep 2.	0.19	0.68	96.19
iTCEs: Rep 3.	0.11	0.4	97.85
hskMPs: Rep 1.	38.96	0.17	59.03
hskMPs: Rep 2.	41.15	1.18	56.13
hskMPs: Rep 3.	39.8	1.11	57.11

Appendix Table S3: Flow cytometry quantification for Appendix Fig S4I. The table shows the results of 3 independent experimental repeats (Rep) in percent of total cells.

Inhibitor type	Control: no inhibitor	MEK inhibitor: PD98059	Notch inhibitor: DAPT	PI3K inhibitor: LY294002	AKT inhibitor: MK-2206
Pax7+: Rep 1.	47.16	4.32	1.87	2.52	6.9
Pax7+: Rep 2.	43.26	4.11	2.01	2.4	3.65
Pax7+: Rep 3.	48.14	4.01	1.81	2.45	3.1
Pax7-: Rep 1.	52.84	95.68	98.13	97.48	93.1
Pax7-: Rep 2.	56.74	95.89	97.99	97.6	96.35
Pax7-: Rep 3.	51.86	95.99	98.19	97.55	96.9

Appendix Table S4: Flow cytometry quantification for Figure 2L-P. The table shows the results of 3 independent experimental repeats (Rep) in percent of total cells.

Inhibitor type	FGF-R inhibitor: PD173074	IGF-1R inhibitor: Tyrphostin
Pax7+: Rep 1.	20.54	4.4
Pax7+: Rep 2.	19.65	4.81
Pax7+: Rep 3.	20.31	4.37
Pax7-: Rep 1.	79.46	95.6
Pax7-: Rep 2.	80.35	95.19
Pax7-: Rep 3.	79.69	95.63

Appendix Table S5: Flow cytometry quantification for Appendix Fig S6C and D. The table shows the results of 3 independent experimental repeats (Rep) in percent of total cells.

Surface marker	Pax7-AF488+ / CD 56 (NCAM)-PE-Cy7+	Pax7-AF488+ / Integrin α9-APC-Cy5.5+	Pax7-AF488+ / CD 271 (NGFR)-PerCP-Cy5.5+	Pax7-AF488+ / CD 82 (Kai-1)-AF647+	Pax7-AF488+ / CD 362 (SDC2)-APC+	Pax7-AF488+ / CD 54 (ICAM)-BV605)	Pax7-AF488+ / CD 34-BV605	Pax7-AF488+ / CD 57 (HNK-1)-PE-CF594	CD 56 (NCAM)-PE-Cy7+ / Integrin α9-APC-Cy5.5	Pax7+ iTCEs
Rep 1.	87.01	88.18	12.88	23.05	71.47	7.87	25.11	8.03	80.88	99.01
Rep 2.	89.58	91.87	8.01	19.55	68.04	5.12	24.77	8.78	81.17	98.13
Rep 3.	84.14	85.04	13.01	23.27	72.36	6.98	24.13	5.63	78.98	99.12

Appendix Table S6: Flow cytometry quantification for Figure 3A-I. The table shows the results of 3 independent experimental repeats (Rep) in percent of total cells.